AIAA JOURNAL
Vol. 33, No. 9, September 1995

Technical Notes

TECHNICAL NOTES are short manuscripts describing new developments or important results of a preliminary nature. These Notes cannot exceed 6 manuscript pages and 3 figures; a page of text may be substituted for a figure and vice versa. After informal review by the editors, they may be published within a few months of the date of receipt. Style requirements are the same as for regular contributions (see inside back cover).

Calculated Effect of Freestream Turbulence on Aerodynamic Characteristics of a Delta Wing

Joachim Pollak* and C. Edward Lan†
University of Kansas, Lawrence, Kansas 66045

Introduction

FREESTREAM turbulence affects the shear layer near a solid surface by changing the boundary-layer thickness, point of transition, separation, and skin friction.[1] It also interacts with the wake to change the shape of it. The shape and location of the leading-edge separated vortex core, its pressure variation, breakdown, or reattachment location are also possible parameters to be affected. Recently, grid-generated turbulence was found to reduce the lift coefficient, lift curve slope, and $C_{L\max}$ of a 76-deg delta wing.[2] More remarkable is the reduction in the magnitude of dihedral effect ($C_{\ell\beta}$). It was also found that the secondary separation line moved more outboard and no tertiary separation line could be found. Furthermore the observations showed a lower crossflow velocity on the upper surface in turbulent freestream. Available data on a cropped arrow wing also show differences in lift and $C_{\ell\beta}$ measured in the 12-ft tunnel[3] and the full-scale tunnel[4] at NASA Langley. These data have been compared in Ref. 5. As reviewed by Erickson,[6] the lift for delta wings with sharp edges remained virtually the same with either laminar or turbulent boundary layers. The reason for this was explained experimentally by Hummel[7] in the reduction of the primary suction peak and increase in suction under the secondary vortex for a laminar boundary layer. These two effects are small for a turbulent boundary layer. Therefore, transition is not the primary reason for the reduction in measured lift in the presence of freestream turbulence.

To use the Reynolds-averaged Navier–Stokes equations in simulation, turbulence modeling is needed. However, there are no simple models available for the effect of freestream turbulence. Most existing turbulence models are for wall-bounded shear flow. Experimently, Pedišius et al.[8] showed that the freestream turbulence penetrated into most of the boundary layer to increase the turbulent level in and outside the boundary layer. In this Note, an algebraic eddy viscosity model for the effect of freestream turbulence will be developed to model the results of Pedišius et al. The purpose is to show that freestream turbulence is one possible source of discrepancy in tunnel data.

Theoretical Approach

Turbulence has viscous terms in all directions that would require an eddy viscosity tensor.[9] All fluctuating terms occur in space derivatives. If "uniform" homogeneous turbulence is assumed, all derivatives are then zero. The thin-layer approximation also means only the eddy viscosity normal to the surface is retained. The two-layer eddy viscosity model of Baldwin–Lomax[10] will be modified by adding the contribution of freestream turbulence.

The freestream turbulence is assumed to have a uniform energy over the boundary-layer region except for the viscous sublayer. Thus a uniform additional eddy viscosity depending only on the turbulence level of freestream is needed. Therefore, a model suggested by Prandtl is appropriate:

$$\mu_t = C_k \rho \ell \sqrt{\bar{k}} \tag{1}$$

The fluctuating energy $\bar{k}$ is directly related to $\overline{u'^2}$. For a homogeneous turbulence, it can be assumed that

$$\sqrt{\bar{k}} \sim \sqrt{\overline{u'^2}} = (Tu)u_\infty \tag{2}$$

which defines the turbulence level Tu. On the other hand, the magnitude of the turbulence level inside a turbulent boundary layer close to the wall is measured to be higher than that of the freestream turbulence.[8] Thus there is a connection between the eddy viscosities of free air and boundary layer. The connecting variable is taken to be the mixing length ℓ. It is assumed that $\ell = C_{CP} y_{\max}$, where $C_{CP} = 1.6$ is a constant used in Ref. 10 and $y_{\max}$ is the y station where the vorticity function $F(y)$ defined therein is maximum. To account for the fluctuations being damped out close to the wall, both the mixing length and fluctuating velocity are multiplied with the factor $\lambda = 1 - \exp(-y^+/A^+)$ from Van Driest. Note that y^+ is a dimensionless distance from the wall. In this study, $A^+ = 26$, as it is used in Ref. 10. The turbulence level is referenced to Mach number to result in the additional eddy viscosity due to freestream turbulence:

$$\mu_{t_{Tu}} = C_k \rho C_{CP} y_{\max} [1 - \exp(-y^+/A^+)]^2 Tu \cdot M \tag{3}$$

As for C_k, a value of 0.01 is used in Ref. 11 for the simulation of turbulent reacting flow. For a k-ε model the constant is $C_\mu = 0.09$. In the present case an approximation for C_k is made by comparing the predicted lift for a 76-deg delta wing with the test data from Ref. 2. For $C_k = 0.045$ the closest match of lift data with experiment at one angle of attack can be made. No attempt to optimize this value of C_k has been done.

Numerical Results

Lift

A 76-deg delta wing with sharp leading edges tested in the BART tunnel of NASA Langley Research Center will first be simulated. This wing model was also treated in Ref. 12 for the tunnel wall interference in the past. In the present calculation, a full turbulent boundary layer is assumed. Figure 1 shows the comparison of lift coefficient computed with the ARC3D solver with the measured data. Up to 30 deg the calculation predicts the correct loss of lift due to freestream turbulence.

Flow Characteristics

The main purpose here is to show some calculated effects of the freestream turbulence that represents one possible source of discrepancy in tunnel data. For this purpose, a 75-deg delta wing located at the center of the octogonal 12-ft tunnel at NASA Langley will be simulated. More detail can be found in Ref. 13.

Received Aug. 15, 1994; revision received March 24, 1995; accepted for publication April 13, 1995.

*Graduate Assistant, Department of Aerospace Engineering.

†Bellows Distinguished Professor of Aerospace Engineering and Center for Excellence in Computer Aided Systems Engineering. Associate Fellow AIAA.

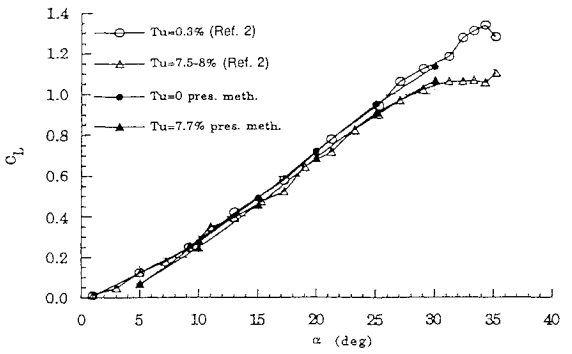

Fig. 1 Lift curve for a 76-deg delta wing in the BART tunnel at M = 0.2 and $Re = 0.5 \times 10^6$.

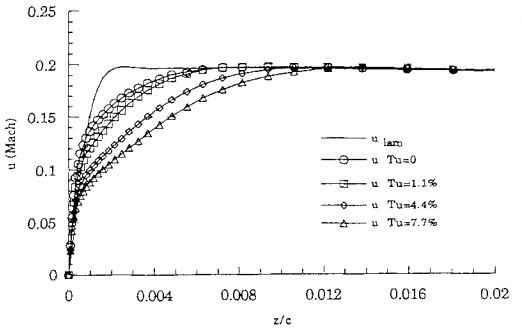

Fig. 2 Streamwise velocity distribution in the boundary layer on the upper surface of a 75-deg delta wing in an octogonal 12-ft tunnel: $x/c = 0.833$, $y = 0$, $\alpha = 20$ deg, $M = 0.2$, and $Re = 10^6$.

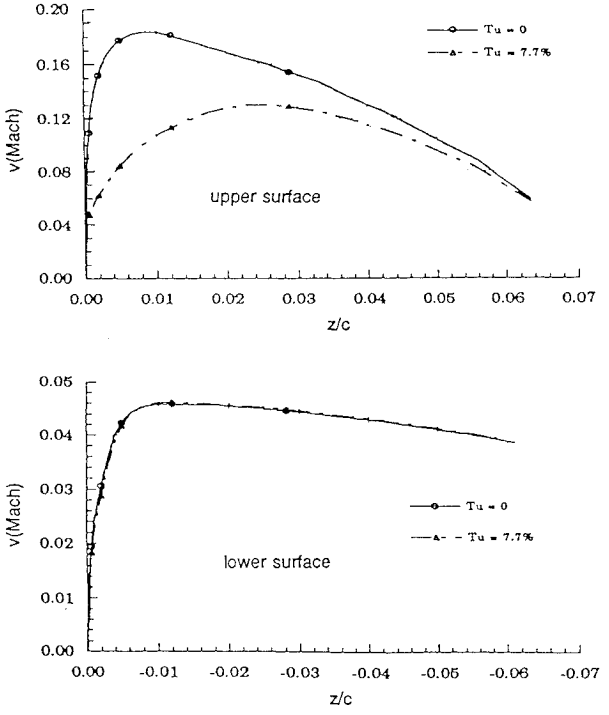

Fig. 3 Spanwise velocity distribution in the boundary layer on the upper surface of a 75-deg delta wing in an octogonal 12-ft tunnel: $x/c = 0.833$, $y/b/2 = 0.578$, $\alpha = 20$ deg, $M = 0.2$, and $Re = 10^6$.

Figure 2 presents the change in the u-velocity distribution in the boundary layer at $\alpha = 20$ deg. With increasing Tu the velocity profile indicates a much thicker boundary layer on the upper surface. The spanwise velocity v has a significant variation (Fig. 3). With increasing Tu, v has a lower slope on the upper surface and no significant changes on the windward side. The calculated lower value of v on the leeward side agrees with the test results of Washburn, who measured a lower crossflow angle for the turbulent freestream.[2]

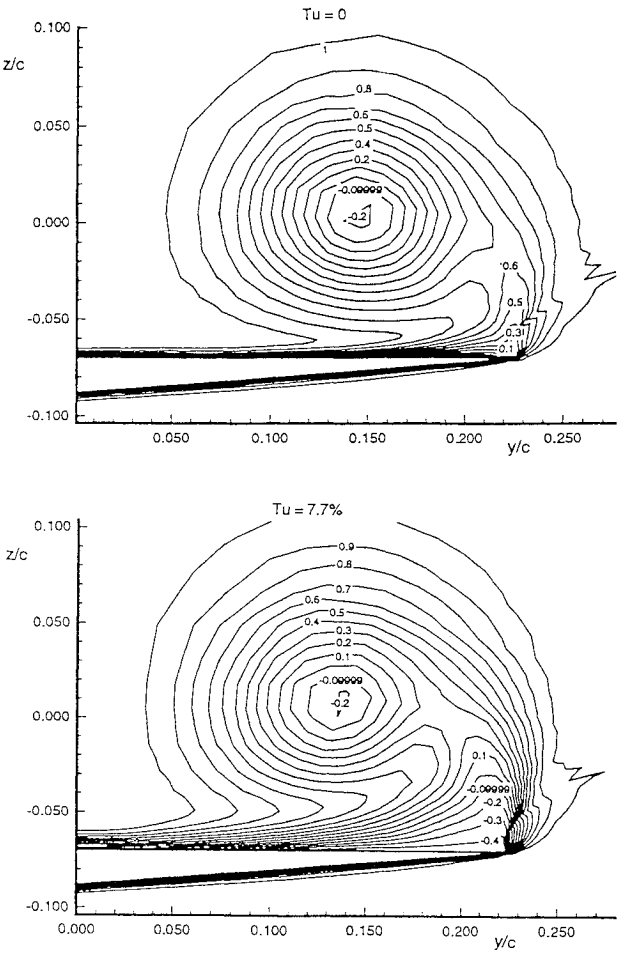

Fig. 4 Total pressure coefficients of a 75-deg delta wing in an octogonal 12-ft tunnel: $x/c = 0.833$, $\alpha = 20$ deg, $M = 0.2$, and $Re = 10^6$.

There were no experimental surface pressures and boundary-layer profiles available for comparison. The total pressure coefficient plots indicate again an overall increase in the boundary-layer thickness (Fig. 4). The increase in boundary-layer thickness tends to push the secondary separation line outward. The total pressure in this outer region is much lower than that with $Tu = 0$. The location of the vortex core and the magnitude of the total pressure there are changed only slightly. The vortex in turbulent freestream is slightly wider. However, the vortex-induced upper-surface pressure is much lower.[13]

Since the present code cannot simulate the asymmetrical flow conditions, an explanation to the change in $C_{\ell\beta}$ can be found in spanwise velocity (Fig. 3). In theory the antisymmetrical loads producing the rolling moment are proportional to the difference of v on the upper and lower surfaces. Since in a turbulent freestream the latter is lower, $C_{\ell\beta}$ becomes less negative.

References

[1]Hinze, J. O., *Turbulence*, 2nd ed., McGraw–Hill, New York, 1975.

[2]Washburn, A. E., "The Effect of Freestream Turbulence on the Vortical Flow over a Delta Wing," M.S. Thesis, George Washington Univ., Washington, DC, Dec. 1990.

[3]Yip, L. P., and Murri, D. G., "Effects of Vortex Flaps on the Low-Speed Aerodynamic Characteristics of an Arrow Wing," NASA TP 1914, Nov. 1981.

[4]Johnson, J. L., Jr., Grafton, S. B., and Yip, L. P., "Exploratory Investigation of the Effects of Vortex Bursting on the High-Angle-of-Attack Lateral-Directional Stability Characteristics of Highly-Swept Wings," AIAA Paper 80-0463, March 1980.

[5]Lan, C. E., and Hsu, C. H., "Effects of Vortex Breakdown on Longitudinal and Lateral-Directional Aerodynamics of Slender Wings by the Suction Analogy," AIAA Paper 82-1385, Aug. 1982.

[6]Erickson, G. E., "Vortex Flow Correlation," International Council of the Aeronautical Sciences, ICAS Paper 82-6.6.1, Aug. 1982, p. 36.

[7]Hummel, D., "On the Vortex Formation over a Slender Wing at Large Angles of Attack," AGARD-CP-247, Oct. 1978.
[8]Pedišius, A., Janušas, V., and Zygmantas, G., "Distortion of the Structure of the Turbulent Boundary Layer by High Free-Stream Turbulence," *Fluid Mechanics Soviet Research*, Vol. 20, No. 5, 1991.
[9]White, F. M., *Viscous Flow Theory*, McGraw–Hill, New York, 1991.
[10]Baldwin, B. S., and Lomax, H., "Thin Layer Approximation and Algebraic Model for Separated Turbulent Flows," AIAA Paper 78-257, Jan. 1978.
[11]Frankel, S. H., Adumitroaie, V., Madnia, C. K., and Givi, P., "Large Eddy Simulation of Turbulent Reacting Flows by Assumed PDF Methods," *Engineering Application to Large Eddy Simulation*, FED-Vol. 162, American Society of Mechanical Engineers, 1993, pp. 81–101.
[12]Thomas, J. P., and Lan, C. E., "The Simulation and Correction of Wind Tunnel Wall Interference on Delta-Wing Lift Using Navier–Stokes and Euler Solutions," AIAA Paper 91-3300, Sept. 1991.
[13]Pollak, J., "Navier–Stokes Simulation of the Influence of Free-Stream Turbulence on the Aerodynamic Characteristics of a Delta Wing," M.S. Thesis, Univ. of Kansas, Lawrence, KS, Dec. 1993.

Transparent Acoustic Source Condition Applied to the Euler Equations

Chang-Jeon Hwang* and Duck-Joo Lee†
Korea Advanced Institute of Science and Technology, Taejon 305-701, Republic of Korea

Nomenclature

e = total energy
$\boldsymbol{F}$ = x-direction flux vector, i.e., $[\rho u, \rho u^2 + p, \rho uv, u(e + p)]^T$
$\hat{\boldsymbol{F}}$ = ξ-direction flux vector
F_2, F_4 = related to the spatial gradient of steady flow flux in the ξ, η direction and the perturbation flux in the η direction, Ref.1
f = frequency
$\boldsymbol{G}$ = y-direction flux vector, i.e., $[\rho v, \rho vu, \rho v^2 + p, v(e + p)]^T$
$\hat{\boldsymbol{G}}$ = η-direction flux vector
J = Jacobian transformation
$\hat{\boldsymbol{P}}, \hat{\boldsymbol{P}}^{-1}$ = matrix by which $\hat{\boldsymbol{U}}$ is related to $\hat{\boldsymbol{W}}$, Ref. 9
$\hat{\boldsymbol{U}}$ = conservative variable vector in the generalized coordinate system
ε = nondimensionalized source strength
τ = real time
τ_ξ = time at fixed ξ

Subscripts

s = sound source
0 = steady flow quantity

Superscripts

$'$ = perturbed quantity
$-$ = dimensional quantity

I. Introduction

RECENTLY, several investigators[1–4] have attempted to simulate acoustic problems numerically by using well-developed numerical schemes. Two approaches have been used for numerical simulations of acoustic problems. One is to use the linearized Euler equations[1,2] and the other is to use nonlinear equations[3,4] of fluid, motion, such as Euler/Navier–Stokes equations. In any approach, the appropriate solvers should be applied because the amplitude of the acoustic wave is small and most problems of aeroacoustics are fully unsteady. Consequently, a numerical solver for acoustic problems should have minimal dissipation and dispersion errors.[5] In addition, unlike the flow problems, inflow/outflow/far-field boundary conditions are critical for accurate long range simulations.[1,2,5]

Acoustic source conditions are also important in the simulation of complex acoustic phenomena, such as the reflection and transmission of an incident wave that might occur wherever there exists an area change, e.g., a rocket nozzle,[6] a muffler, or a cascade stator and rotor, etc. Thompson's idea[7] is employed for the nonreflecting boundary conditions and two kinds of acoustic source conditions, which are compatible with the nonreflecting boundary condition, are compared in this paper; one is similar to the condition implemented by Watson and Myers[1] and the other is proposed here, which also has nonreflecting properties in the source model. The source models are tested for a uniform duct with a primary source located to the right and with a secondary source located to the left.

II. Boundary and Acoustic Source Conditions

We choose the strong conservative form of two-dimensional Euler equations of inviscid gas dynamics as governing equations. Conventional numerical schemes for the Euler equations are employed, using an upwind finite difference formulation[8] and Runge–Kutta time stepping.[9] The numerical flux is based on Roe's approximate Riemann solver with an entropy fix.[8] Higher order schemes can be constructed from MUSCL.[8] In addition, the slope limiter function, called Koren's differentiable limiter, is used to prevent the numerical solution from oscillations.[8] Based on this numerical scheme for the governing equations, the nonreflecting boundary condition and the two source conditions are described.

A. Nonreflecting Boundary Conditions

First we will briefly describe Thompson's boundary condition,[7] which is closely related to the acoustic source condition to be described later. At the inlet or outlet boundary of $\xi = \text{const}$ as shown in Fig. 1, the wave can be considered as one dimensional so that

$$\partial_{\tau_\xi} \hat{\boldsymbol{U}} + \partial_\xi \hat{\boldsymbol{F}} = 0 \tag{1}$$

Then, using Eq. (1), we can rewrite the two-dimensional Euler equations at the ξ boundary as[7]

$$\partial_\tau \hat{\boldsymbol{U}} + \partial_\eta \hat{\boldsymbol{G}} = -\partial_\xi \hat{\boldsymbol{F}} = \partial_{\tau_\xi} \hat{\boldsymbol{U}} \tag{2}$$

where

$$\hat{\boldsymbol{U}} = (\rho, \rho u, \rho v, e)^T / J$$

$$\hat{\boldsymbol{F}} = (\xi_x \boldsymbol{F} + \xi_y \boldsymbol{G}) / J$$

$$\hat{\boldsymbol{G}} = (\eta_x \boldsymbol{F} + \eta_y \boldsymbol{G}) / J$$

We must evaluate the terms $\partial \hat{\boldsymbol{U}} / \partial \tau_\xi$ in order to integrate in time at the boundaries. The terms $\partial \hat{\boldsymbol{U}} / \partial \tau_\xi$ can be obtained from Eq. (1) by diagonalizing the flux Jacobian matrix $\hat{\boldsymbol{A}} = \partial \hat{\boldsymbol{F}} / \partial \hat{\boldsymbol{U}}$ as

$$\partial_{\tau_\xi} \hat{\boldsymbol{W}} + \hat{\Lambda} \partial_\xi \hat{\boldsymbol{W}} = 0 \tag{3}$$

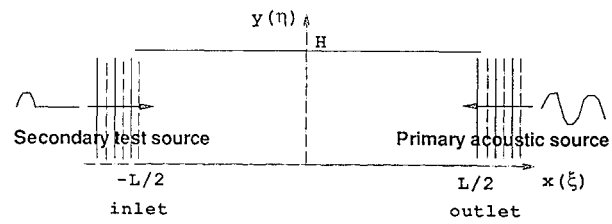

Fig. 1 Schematic diagram and coordinate system of a uniform duct.

Received Nov. 20, 1994; revision received March 20, 1995; accepted for publication April 17, 1995.

*Graduate Student, Department of Aerospace Engineering. 373-1, Kusong-dong, Yusong-gu.
†Associate Professor, Department of Aerospace Engineering, 373-1, Kusong-dong, Yusong-gu. Member AIAA.